

# Immobilization of Horseradish Peroxidase on Multi-Armed Magnetic Graphene Oxide Composite: Improvement of Loading Amount and Catalytic Activity

Junhui Rong<sup>1</sup>, Zijuan Zhou<sup>2</sup>, Yun Wang<sup>1\*</sup>, Juan Han<sup>3</sup>, Chunmei Li<sup>1</sup>, Wenli Zhang<sup>1</sup> and Liang Ni<sup>1</sup>

<sup>1</sup>School of Chemistry and Chemical Engineering, Jiangsu University, 212013 Zhenjiang, PR China

<sup>2</sup>School of Food Science and Nutrition, University of Leeds, Leeds, LS2 9JT, UK

<sup>3</sup>School of Food and Biological Engineering, Jiangsu University, 212013 Zhenjiang, PR China

Received: 6 May 2018

Accepted: 8 May 2019



\*Corresponding author:

Phone: +8615896385156

E-mail: [yunwang@ujs.edu.cn](mailto:yunwang@ujs.edu.cn)

## SUMMARY

In this study, a novel type of multi-armed polymer (polyethylene glycol, PEG) magnetic graphene oxide (GO) composite (GO@Fe<sub>3</sub>O<sub>4</sub>@6arm-PEG-NH<sub>2</sub>) has been synthesized as a support for immobilization of horseradish peroxidase (HRP) for the first time. The loading amount of HRP was relatively high (186.34 mg/g) due to the surface of carrier material containing a large amount of amino groups from 6arm-PEG-NH<sub>2</sub>, but degradation rate of phenols was also much higher (95.4 %), which is attributed to the synergistic effect between the free HRP (45.4 %) and the support material of GO@Fe<sub>3</sub>O<sub>4</sub>@6arm-PEG-NH<sub>2</sub> (13.6 %). Compared with the free enzyme, thermal, storage and operational stability of the immobilized HRP improved. The immobilized HRP still retained over 68.1 % activity after being reused 8 times. These results suggest that the multi-armed magnetic composite has good application prospect for enzyme immobilization.

**Key words:** immobilized enzyme, graphene oxide, multi-armed polymer, horseradish peroxidase, synergistic effect

## INTRODUCTION

Horseradish peroxidase (HRP) is a promising biocatalyst, and there are reports that it can be used for the removal of phenolic compounds, hormones, aromatic amines and the decolourization of textile wastewater (1–3). In the presence of hydrogen peroxide, HRP can catalyze the oxidation of phenols to produce phenoxy radical. The resulting free radicals voluntarily form insoluble polymers that can be separated by simple filtration or decantation. However, one of the major drawbacks of this method is that the catalytic activity of HRP involved in the reaction is lower because of the inactivation of the enzyme in the polymerization process (4). In order to solve this problem, Cheng *et al.* (5) reported that the immobilized enzyme can improve the degradation efficiency of the phenols.

Enzyme immobilization is widely used in the field of biocatalysis and biosensors. Common immobilized materials contain SiO<sub>2</sub> (6), polysaccharide derivatives (7), chitosan (8), Fe<sub>3</sub>O<sub>4</sub> magnetic nanoparticles (9), graphene oxide (10) and so on. Graphene oxide (GO) is a two-dimensional nanomaterial with a thickness of only one atom. Because it is rich in surface groups and has a relatively large functional surface area with a unique double-sided structure, GO can be used as a support for biological macromolecules (11,12). However, an enzyme immobilized on the GO cannot be recycled, but GO@Fe<sub>3</sub>O<sub>4</sub> can easily be separated from the solution using an additional magnetic field. At the same time, GO and Fe<sub>3</sub>O<sub>4</sub> have been reported to possess peroxidase-type enzyme activity (13–15). Therefore, the hydrogen peroxide, GO and Fe<sub>3</sub>O<sub>4</sub> can all catalyze the oxidation of peroxidase substrate 3,3',5,5'-tetramethylbenzidine.

The 6arm-PEG-NH<sub>2</sub> is a polyethylene glycol derivative which is used to modify the protein polypeptide. Since it is rich in amino groups, it can form an immobilized enzyme through the crosslinking agent glutaraldehyde binding with protein and increase the stability and loading amount of enzyme (16), but it can also react with the carboxyl group of materials (such as polyacrylic acid) to form stable amide bond, which improves the solubility and

stability of the material. Herein, a new magnetic multi-armed nanocomposite ( $\text{GO@Fe}_3\text{O}_4@6\text{arm-PEG-NH}_2$ ) was designed. On the one hand, GO and  $\text{Fe}_3\text{O}_4$ , with the peroxidase-like activity, can synergize with the HRP to enhance the degradation of phenols. On the other hand, 6arm-PEG contains a large number of amino groups, which can greatly increase the loading amount of the enzyme. Hydrophilic PEG can contribute to the ability of the enzyme to retain more of the essential water molecules, to prevent the inactivation induced by polymerization precipitation and to maintain its active conformation.

In this work, the magnetic composite  $\text{GO@Fe}_3\text{O}_4@6\text{arm-PEG-NH}_2$  was synthesized and used to immobilize HRP. In such a system, multiple effects are anticipated. Firstly, GO and  $\text{Fe}_3\text{O}_4$  are artificial enzyme-like materials. Secondly, the magnetic properties of the  $\text{Fe}_3\text{O}_4$  nanoparticles allow the enzyme immobilized on the composite to be easily separated from the solution by an additional magnetic field, thereby reducing the cost of enzyme use. Thirdly, the loading capacity of immobilized HRP was improved because the surface of GO is grafted with a large number of amino-containing polymers bound by covalent bonds. Therefore, we investigated the catalytic activity of immobilized HRP for the degradation of phenols at different pH and temperature and compared it to its free form. Additionally, we investigated the thermal stability, storage stability and reusability of immobilized HRP, the effect of different reaction parameters on the degradation rate of phenols, and the optimum reaction parameters of the immobilized enzyme.

## MATERIALS AND METHODS

### Materials

Potassium permanganate, barium chloride, hydrochloric acid, chloroacetic acid, ethanol, ammonium hydroxide aqueous solution (25 %, by mass), iron(II) sulfate heptahydrate, hydrogen peroxide, sodium dihydrogen phosphate, disodium phosphate, glutaraldehyde, sulfuric acid, phenol, 4-aminoantipyrine (4-AAP) and sodium hydroxide were obtained from Sinopharm Chemical Reagent Co., Ltd (Shanghai, PR China). Iron(III) chloride hexahydrate, polyethylene glycol (PEG), graphite and sodium nitrate were bought from Aladdin Industrial Corporation (Shanghai, PR China). The 6arm-PEG-NH<sub>2</sub> was supplied by Shanghai Jinpan Biotech Co., Ltd. (Shanghai, PR China). Horseradish peroxidase (HRP) was bought from Shanghai Jinsui Biotechnology Co., Ltd (Shanghai, PR China). The 1-(3-dimethylaminopropyl)-3-ethylcarbodiimide hydrochloride (EDAC) was bought from Sangon Biotech Co., Ltd (Shanghai, PR China). All other reagents were of analytical grade and used without any further treatment. Deionized water was used in all the experiments.

### Synthesis of GO-COOH

Graphene oxide (GO) was synthesized using Hummers method (17). Masses of 0.5 g graphite and 0.5 g  $\text{NaNO}_3$  were

added to the concentrated  $\text{H}_2\text{SO}_4$  (12 mol/L, 23 mL) solution and stirred at 600 rpm on a mechanical agitator in ice bath for 15 min. After slowly adding 4.0 g of  $\text{KMnO}_4$ , the mixture was transferred to a water bath heated to 40 °C and stirred (JJ-1; Xinrui Apparatus Factory, Jintan, PR China) at 600 rpm for 90 min. A volume of 50 mL of deionized water was added to the reaction system and stirred for 10 min. After adding 6 mL of hydrogen peroxide, the colour of the mixture changed from purple to golden. After standing for 24 h, the supernatant was decanted, the precipitate was collected by suction filtration and washed repeatedly with 5 % hydrochloric acid until no precipitate was detected in the supernatant with  $\text{BaCl}_2$ . The precipitate was then washed with deionized water and centrifuged (TGL-16aR; Shanghai Anting Scientific Instrument Factory, Shanghai, PR China) at 8000×g until the pH of the supernatant reached pH=7. It was then placed in a cuvette and dried in a vacuum oven (DZF-6021; Shanghai Yiheng Instruments Co., Ltd, Shanghai, PR China) to constant mass. Next, to 1.0 g of the above product 0.4 g NaOH and 200 mL water were added and the mixture was ultrasonicated (KQ-250B; Kunshan Ultrasonic Instruments Co., Ltd, Kunshan, PR China) for 2 h. Then, 0.5 to 0.6 g of chloroacetic acid was added and ultrasonicated for 2 h. The solution was centrifuged at 8000×g, washed repeatedly with deionized water to neutral pH and dried in a vacuum oven to constant mass to obtain GO-COOH, which is rich in carboxyl groups on the surface.

### Synthesis of $\text{GO@Fe}_3\text{O}_4$

$\text{Fe}_3\text{O}_4$  was synthesized on the surface of GO-COOH by coprecipitation (18,19). A mass of 0.2 g of GO-COOH was dispersed in 100–150 mL of water, then 0.466 g of  $\text{FeCl}_3\cdot 6\text{H}_2\text{O}$  and 0.48 g of  $\text{FeSO}_4\cdot 7\text{H}_2\text{O}$  were added and ultrasonicated (KQ-250B; Kunshan Ultrasonic Instruments Co., Ltd.) for 10 min. The temperature of the mixture was raised to 60 °C and 20 mL of aqueous ammonia (3.5 mol/L) were added and reacted for 60 min. The product was separated with a magnet, washed with deionized water to neutral pH and then dried to constant mass in an oven (DHG-9077; Taicang Jinghong Experimental Equipment Co., Ltd, Taicang, PR China) to obtain magnetic graphene oxide  $\text{GO@Fe}_3\text{O}_4$ .

### Synthesis of $\text{GO@Fe}_3\text{O}_4@6\text{arm-PEG-NH}_2$

According to a previous report (20), the improved method of 6arm-PEG-NH<sub>2</sub> grafting was applied in this study. A mass of 200 mg of  $\text{GO@Fe}_3\text{O}_4$  together with 20 mL of 6arm-PEG-NH<sub>2</sub> were added to 200 mL of deionized water and sonicated (KQ-250B; Kunshan Ultrasonic apparatus Co., Ltd.) for 1 h. After adding 40 mg of EDAC to the solution, the mixture was stirred for 2 h at room temperature and then 52 mg of EDAC were added. Stirring continued for 12 h, then the product was separated by an external magnetic field, washed with deionized water to neutral pH, and then dried under vacuum (DHG-9077; Taicang Jinghong Experimental Equipment Co., Ltd) at 40 °C.

### Characterization of GO@Fe<sub>3</sub>O<sub>4</sub>@6arm-PEG-NH<sub>2</sub>

The chemical structure of the magnetic material was determined by a Fourier transform infrared (FTIR) spectrometer (Nexus 470; Thermo Fisher Scientific, Madison, WI, USA) using KBr pellets, and the diffuse reflectance spectra were scanned over the range of 400–4000 cm<sup>-1</sup>. The morphology of each step product was detected by transmission electron microscopy (Tecnai™ 12; FEI Company, Hillsboro, OR, USA). During the test, the sample was dispersed in ethanol and spotted onto a carbon-coated copper mesh and then dried at room temperature. The magnetization curves of GO@Fe<sub>3</sub>O<sub>4</sub> and GO@Fe<sub>3</sub>O<sub>4</sub>@6arm-PEG-NH<sub>2</sub> were measured by vibrating sample magnetometer (VSM 7410; Lake Shore Cryotronics, Inc., Westerville, OH, USA) at room temperature. The X-ray photoelectron spectroscopy (XPS) measurements were performed using a hemispherical analyzer (ESCALAB™ 250Xi; Thermo Fisher Scientific, Waltham, MA, USA) equipped with Al K $\alpha$  radiation as X-ray source ( $k=100$  eV).

### Immobilization of HRP on GO@Fe<sub>3</sub>O<sub>4</sub>@6arm-PEG-NH<sub>2</sub>

A mass of 100 mg of magnetic material was added to 100 mL of glutaraldehyde solution and shaken on vortex mixer (HB20; Hangzhou Longyang Scientific Apparatus Co., Ltd., Hangzhou, PR China) at 50 °C and 200 rpm for 6 h. The magnetic material was separated from the solution with a magnet and dried in vacuum oven (DZF-6020; Shanghai Yiheng Scientific Apparatus Co., Ltd., Shanghai, PR China). The magnetic material was prepared as a suspension with 0.2 M phosphate-buffered saline (PBS; pH=7.0). The HRP solution was added to the suspension and mixed uniformly. The mixture was incubated at constant temperature for 120 min and the immobilized HRP was separated with a magnet. The concentration of the enzyme in the supernatant after separation was examined. The support material was rinsed twice with a buffer solution to remove free HRP. The concentration of residual HRP in the supernatant solution was detected using UV-Vis spectrophotometer (UV-2450; Shimadzu, Tokyo, Japan), according to the Bradford protein assay method (21). The loading mass of HRP ( $Q$ /(mg/g)) can be calculated by the following equation:

$$Q = \frac{m_1 - m_2}{m} \quad /1/$$

where  $m_1$  is the protein mass (mg) added to the solution,  $m_2$  is the protein mass (mg) in the remaining supernatant, and  $m$  is the mass (g) of the support material.

### Determination of HRP activity

Enzyme activity was assayed using the traditional Worthington method (22). A volume of 1.4 mL of 4-AAP, 100  $\mu$ L of immobilized HRP solution and 1.5 mL of H<sub>2</sub>O<sub>2</sub> solution were added to the cuvette at 25 °C. The absorbance was measured at 510 nm with a UV-Vis spectrophotometer (UV-2450; Shimadzu) each minute until the increase in the absorbance per

minute remained the same. The enzyme activity (EA/(U/mL)) was calculated according to the following equation:

$$EA = \frac{A_{510\text{nm}} \cdot V_t}{10 \cdot 0.685 \cdot V_e} \quad /2/$$

where  $A_{510\text{nm}}$  denotes the increase of absorbance per minute at 510 nm,  $V_t$  is the total volume of the reaction solution (3 mL in this experiment),  $V_e$  is the volume of free or immobilized enzyme HRP (0.1 mL in this experiment), 10 is the number of dilutions of the sample and 0.685 is the increase of the absorbance of a unit of horseradish peroxidase in 1 minute.

### Evaluation of phenol degradation

The reaction solution (pH=7.0) contained 100 mg/L phenols, 0.2 mg/L immobilized enzyme, 200 mmol/L PBS, H<sub>2</sub>O<sub>2</sub> (the molar ratio of H<sub>2</sub>O<sub>2</sub>/phenol was set at 1) and PEG (the mass ratio of PEG/phenol was set at 0.4) (23). After completion of the reaction, it was quenched by the addition of concentrated sulfuric acid. The solution was made up to 10 mL with PBS (pH=7.0). The immobilized HRP was collected by magnet adsorption. The supernatant was filtered and the phenol concentration was measured. The equation for calculating the degradation rate of phenols ( $DR_p$ /% ) is as follows:

$$DR_p = \frac{V \cdot (Y_p^1 - Y_p^2)}{V \cdot Y_p^1} \quad /3/$$

where  $Y_p^1$  is the concentration of phenols in the initial solution (mg/L),  $Y_p^2$  is the concentration of phenols in the remaining liquid (mg/L), and  $V$  is the volume of the reaction solution (L).

## RESULTS AND DISCUSSION

### Preparation and characterization of GO@Fe<sub>3</sub>O<sub>4</sub>@6arm-PEG-NH<sub>2</sub>

**Fig. 1** shows the preparation process of the magnetic material. First, the graphite was oxidized to monolayer graphene oxide. Then the surface of the graphene oxide was carboxylated and the carboxylation of GO with Fe<sub>3</sub>O<sub>4</sub> was carried out on this basis. Then, the 6arm-PEG-NH<sub>2</sub> was grafted onto the surface of the carboxylated graphene oxide by the reaction of the carboxyl group with the amino group. After that, the amino group of the support material and the amino group of the HRP were connected by glutaraldehyde to form an immobilized HRP.

**Fig. 2a** shows the FTIR spectra of GO, GO@Fe<sub>3</sub>O<sub>4</sub> and GO@Fe<sub>3</sub>O<sub>4</sub>@6arm-PEG-NH<sub>2</sub>. GO gave several strong characteristic peaks corresponding to the oxygen functionalities, such as the CO stretching vibration peak at 1732 cm<sup>-1</sup>, O-H bending and stretching vibration in the C-OH groups at 1404 and 3415 cm<sup>-1</sup>. The absorption peak at 573 cm<sup>-1</sup> for GO@Fe<sub>3</sub>O<sub>4</sub> (**Fig. 2a**) was attributed to the iron oxide on the GO surface. The absorption peaks at 1083, 1579 and 2879 cm<sup>-1</sup> (**Fig. 2a**) were assigned to

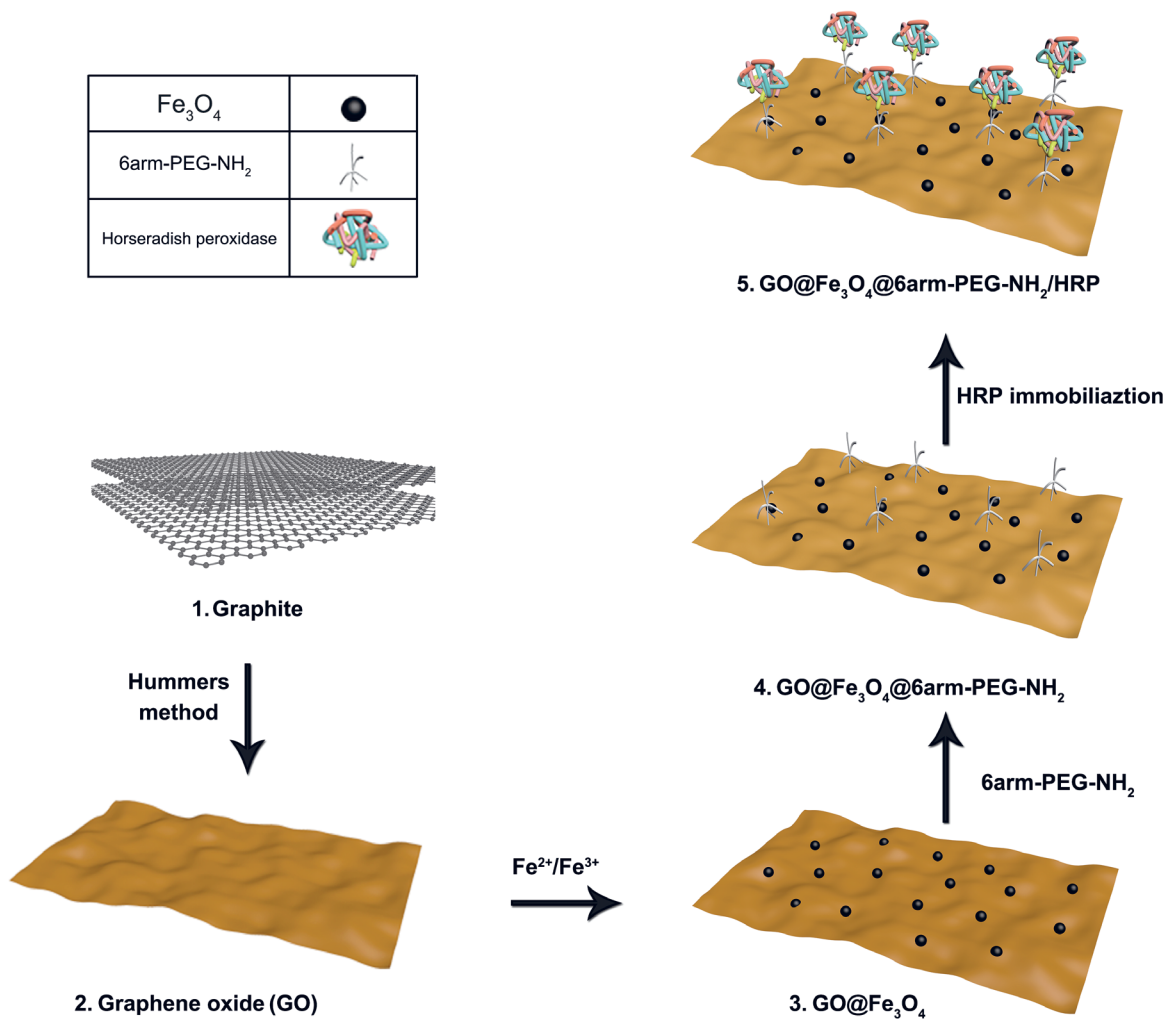


**Fig. 1.** Schematic diagram of immobilization of horseradish peroxidase (HRP) on  $\text{GO@Fe}_3\text{O}_4@6\text{arm-PEG-NH}_2$ . PEG=polyethylene glycol

the vibrations of C-O, N-H and C-H in 6arm-PEG-NH<sub>2</sub> respectively, which demonstrated that 6arm-NH<sub>2</sub> had been grafted onto  $\text{GO@Fe}_3\text{O}_4$ . Compared to the spectrum for  $\text{GO@Fe}_3\text{O}_4@6\text{arm-PEG-NH}_2$ , the spectrum for  $\text{GO@Fe}_3\text{O}_4@6\text{arm-PEG-NH}_2/\text{HRP}$  had additional peaks at 1400–1600  $\text{cm}^{-1}$  for –CONH, and 2800–3000  $\text{cm}^{-1}$  for –CH<sub>2</sub> and –CH<sub>3</sub>. Moreover, the  $\text{GO-Fe}_3\text{O}_4@6\text{arm-PEG-NH}_2/\text{HRP}$  spectrum shows peak shift (1400–1600  $\text{cm}^{-1}$ ) compared to HRP spectrum, indicating that HRP was immobilized *via* covalent bonding. **Fig. 2b** shows the X-ray diffraction (XRD) patterns of GO,  $\text{GO@Fe}_3\text{O}_4$  and  $\text{GO@Fe}_3\text{O}_4@6\text{arm-PEG-NH}_2$ . The diffraction peak characteristic of GO appeared at around  $2\theta=10^\circ$ . Six peaks at 30.1, 35.5, 43.1, 53.4, 57.0 and 62.6° correspond to crystal values of  $\text{Fe}_3\text{O}_4$  given by the International Centre for Diffraction Data (ICDD) (24) file (card no. 19-629) indexed as (220), (311), (400), (422), (511), (440), respectively. The  $\text{Fe}_3\text{O}_4$  crystal form did not change during the reaction.

The specific magnetization values ( $\sigma$ ) of the samples  $\text{GO@Fe}_3\text{O}_4$  and  $\text{GO@Fe}_3\text{O}_4@6\text{arm-PEG-NH}_2$  were 39.61 and 30.80  $\text{A}\cdot\text{m}^2/\text{kg}$ , respectively (**Fig. 2c**). There was no significant residual

magnetic and coercive force at room temperature, indicating that it had superparamagnetic properties. The specific magnetization values were high enough to allow immobilized HRP to be quickly and efficiently separated from the solution.

Components of the composite were measured by thermogravimetric analysis (TGA), and the results are in **Fig. 2d**. The organic components were decomposed and inorganic components were retained with the increase of temperature during TGA. The 74.5 % (by mass) loss of GO microspheres was attributed to the mass ratio of free water and oxygen-containing group of the GO. After binding with  $\text{Fe}_3\text{O}_4$ , the 23.1 % loss of  $\text{GO@Fe}_3\text{O}_4$  was assigned to the physically adsorbed water and oxygen-containing group of the GO. When the 6arm-PEG-NH<sub>2</sub> was introduced, the mass loss of the composite microspheres was about 52.7 %, which was much higher than of  $\text{GO@Fe}_3\text{O}_4$ . The first mass loss (14.4 %) at temperatures up to 200 °C was due to the evaporation of the physically adsorbed water or solvent, and the second major mass loss (38.3 %) at temperatures from 200 to 800 °C was due to

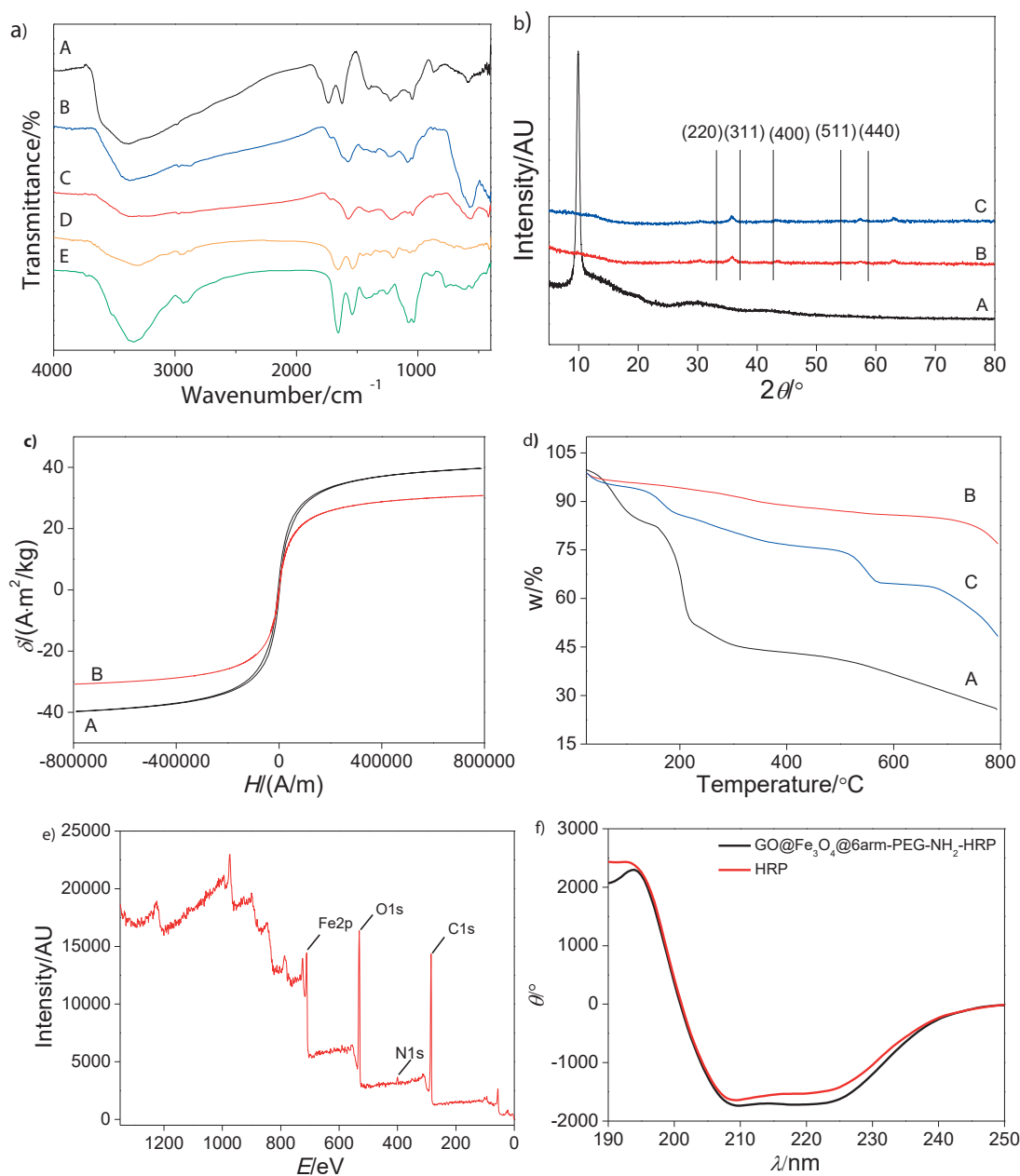


**Fig. 2.** FTIR spectra of: a) A=graphene oxide (GO), B=GO@Fe<sub>3</sub>O<sub>4</sub>, C=GO@Fe<sub>3</sub>O<sub>4</sub>@6arm-PEG-NH<sub>2</sub>, D=GO@Fe<sub>3</sub>O<sub>4</sub>@6arm-PEG-NH<sub>2</sub>/HRP and E=horseradish peroxidase (HRP), b) X-ray diffraction (XRD) patterns of: A=GO-COOH, B=GO@Fe<sub>3</sub>O<sub>4</sub> and C=GO@Fe<sub>3</sub>O<sub>4</sub>@6arm-PEG-NH<sub>2</sub>, c) magnetization curves, specific magnetization  $\sigma$  vs magnetic field strength  $H$ , of: A=GO@Fe<sub>3</sub>O<sub>4</sub> and B=GO@Fe<sub>3</sub>O<sub>4</sub>@6arm-PEG-NH<sub>2</sub>, d) thermogravimetric analysis (TGA) curves of: A=GO, B=GO@Fe<sub>3</sub>O<sub>4</sub> and C=GO@Fe<sub>3</sub>O<sub>4</sub>@6arm-PEG-NH<sub>2</sub>, e) X-ray photoelectron spectroscopy (XPS) spectrum of: GO@Fe<sub>3</sub>O<sub>4</sub>@6arm-PEG-NH<sub>2</sub>, and f) circular dichroism spectrum of HRP and GO@Fe<sub>3</sub>O<sub>4</sub>@6arm-PEG-NH<sub>2</sub>/HRP. PEG=polyethylene glycol

the decomposition of the polymer component 6arm-PEG-NH<sub>2</sub> and GO of the multi-armed magnetic graphene oxide composite.

**Fig. 2e** shows the X-ray photoelectron spectroscopy (XPS) spectrum of the GO@Fe<sub>3</sub>O<sub>4</sub>@6arm-PEG-NH<sub>2</sub> magnetic material. The spectrum of C1s was dominated by a peak around 286.4 eV, which is assigned to graphene carbon, and the spectrum of Fe2p can also be found in the XPS spectrum, indicating the successful synthesis of GO@Fe<sub>3</sub>O<sub>4</sub>. The broad

peaks around 711.2 and 734.3 eV were typical for magnetite, confirming the formation of Fe<sub>3</sub>O<sub>4</sub>. The spectrum of N1s was dominated by a peak around 396.6 eV, which is associated with 6arm-PEG-NH<sub>2</sub>.

To explore the secondary structural changes of HRP after immobilization on GO@Fe<sub>3</sub>O<sub>4</sub>@6arm-PEG-NH<sub>2</sub>, the circular dichroism (CD) spectra of HRP and GO@Fe<sub>3</sub>O<sub>4</sub>@6arm-PEG-NH<sub>2</sub>/HRP were recorded from 190 nm to 250 nm (**Fig. 2f**). Two negative peaks at 208 and 222 nm are observable, which

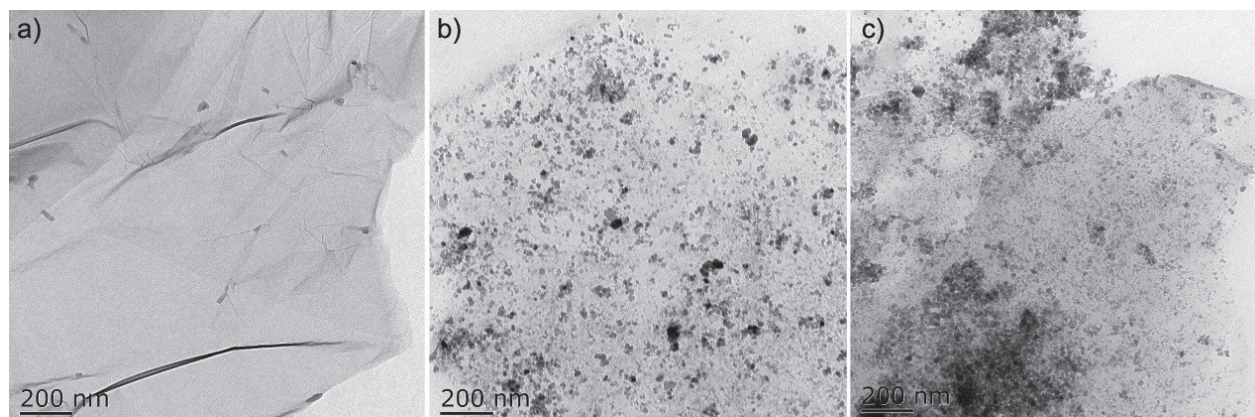


**Fig. 3.** Transmission electron microscopy (TEM) images of: a) GO-COOH, b) GO@Fe<sub>3</sub>O<sub>4</sub> and c) GO@Fe<sub>3</sub>O<sub>4</sub>@6arm-PEG-NH<sub>2</sub>. GO=graphene oxide, PEG=polyethylene glycol

are typical for  $\alpha$ -helical structure of the enzyme, a common characteristic of all HRP, while a positive peak at around 196 nm was assigned to  $\beta$ -sheet structure. Compared with HRP, the secondary structure of GO@Fe<sub>3</sub>O<sub>4</sub>@6arm-PEG-NH<sub>2</sub>/HRP did not significantly change. This shows that the immobilization had no drastic effect on the secondary structure of HRP.

**Fig. 3** shows transmission electron microscopy (TEM) images of the acquired magnetite support material. TEM image of GO-COOH (**Fig. 3a**) shows that it has lamellar structure with obvious folds on the surface, which could provide attachment sites for Fe<sub>3</sub>O<sub>4</sub> nanoparticles and prevent the mutual agglomeration of nanoparticles, as reported in the literature (25). Fe<sub>3</sub>O<sub>4</sub> nanoparticles can be uniformly dispersed on the surface of GO (**Fig. 3b**). Statistical analysis showed that the average size of Fe<sub>3</sub>O<sub>4</sub> particles was (20 $\pm$ 5) nm. Comparing, TEM image of GO@Fe<sub>3</sub>O<sub>4</sub>@6arm-PEG-NH<sub>2</sub> (**Fig. 3c**) shows a large shadow, representing the surface of magnetic GO covered with a layer of polymer, which indicated the successful modification of 6arm-PEG-NH<sub>2</sub>.

#### Optimization of immobilization conditions

The amino group of the enzyme molecule and the amino group of the magnetic material GO@Fe<sub>3</sub>O<sub>4</sub>@6arm-PEG-NH<sub>2</sub> can be ligated by glutaraldehyde, but the high concentration of glutaraldehyde can also lead to inactivation of the enzyme or cause self-crosslinking of the enzyme molecule. Therefore, it is necessary to find the appropriate concentration of glutaraldehyde. **Fig. 4a** shows that when the glutaraldehyde was not added, the loading of HRP was 13.15 mg/g, which indicated that the physical adsorption of the enzyme to the support material was weak. In order to immobilize the enzyme more firmly, the binding force between the two can be enhanced by the addition of a crosslinking agent. When the concentration of glutaraldehyde was increased from 0.05 to 0.10 mol/L, the loading of HRP increased from 95.17 to 143.13 mg/g. However, when glutaraldehyde concentration continued to rise, the loading of HRP was almost unchanged. With the increase of glutaraldehyde concentration, the phenomenon

of self-crosslinking between the enzyme molecules was exacerbated and the enzyme molecules did not bind to GO@Fe<sub>3</sub>O<sub>4</sub>@6arm-PEG-NH<sub>2</sub> anymore, resulting in a slight decrease in the loading of enzyme. Therefore, the optimal concentration of glutaraldehyde was 0.10 mol/L.

**Fig. 4b** shows the effect of the concentration of support material on the immobilization; the loading of the enzyme first increased, and then decreased. The average loading of HRP was 187.47 mg/g when the concentration of support material was lower than 7 mg/L, which may be due to the fact that HRP was almost completely immobilized at these concentrations. Therefore, the optimal concentration of support material was determined to be 7 mg/L.

Different ambient temperatures, ranging from 20 to 50 °C, were tested. **Fig. 4c** shows that with the increase of ambient temperature, the loading of HRP increased. When the temperature was 35 °C, the loading of HRP reached the maximum value of 189.99 mg/g. However, when the temperature was higher than 35 °C, the loading of HRP decreased slightly. Therefore, 35 °C was chosen as the optimal ambient temperature.

Finally, different reaction times were investigated. **Fig. 4d** shows that the loading of immobilized HRP increased with time ranging from 30 to 120 min. It reached a steady value of 180.47 mg/g after 120 min. It can be seen that the immobilization reaction was almost balanced at 120 min. Thus, the optimal reaction time was set at 120 min.

To sum up, under the optimal immobilization conditions (concentration of glutaraldehyde 0.1 mol/L, concentration of support material 7 mg/L, temperature 35 °C and incubation time 120 min), the average loading of HRP was 186.34 mg/g; relative standard deviation (RSD)=0.879 %. However, the activity of the immobilized HRP was about 45.59 U/mg, which equaled only 76.9 % of initial activity. In addition, the loading of immobilized HRP was comparably higher than previously reported supports for HRP (**Table 1** (26–30)). All the above shows that the loading of immobilized HRP on GO@Fe<sub>3</sub>O<sub>4</sub> can be effectively improved by grafting 6arm-PEG.

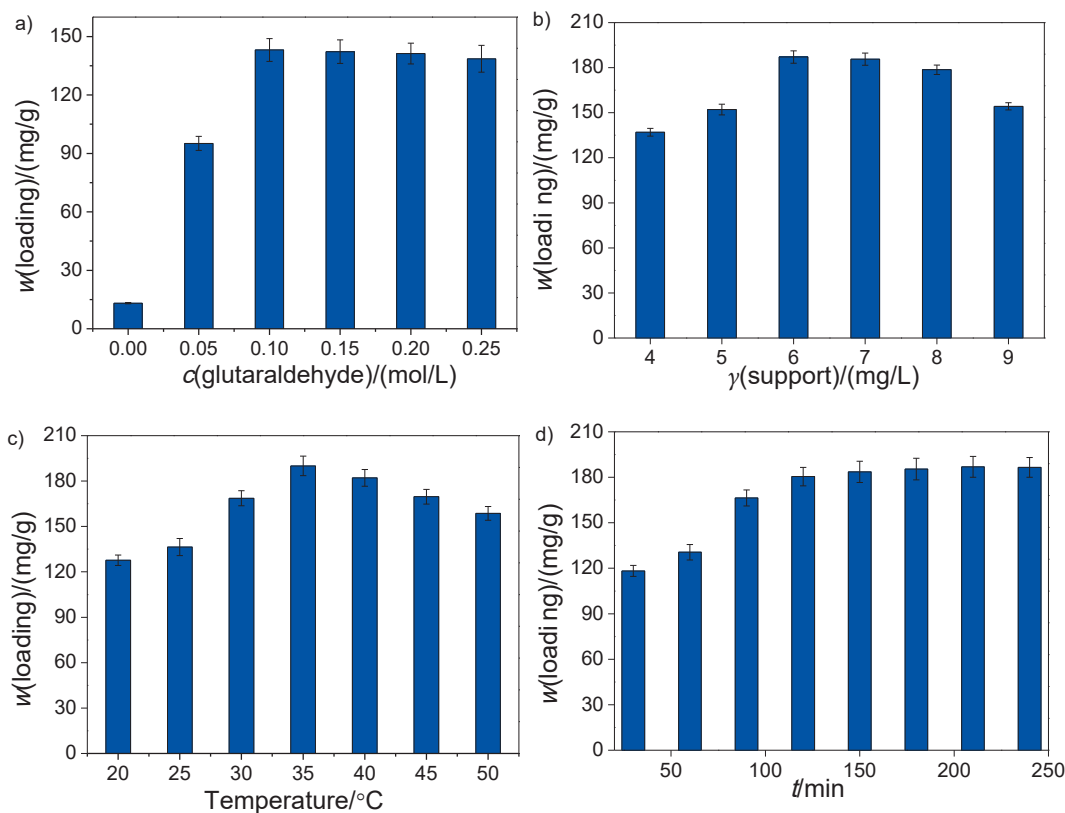


**Fig. 4.** Effect of: a) molar concentration of glutaraldehyde, b) mass concentration of support material, c) temperature and d) reaction time on horseradish peroxidase (HRP) loading

**Table 1.** The loading of previously reported supports for horseradish peroxidase

Support material	w/(mg/g)	Reference
GO/Fe <sub>3</sub> O <sub>4</sub>	0.7	(26)
Porous aminopropyl glass beads	9.6	(27)
Alkylamine glass	18.4	(28)
Alkylamine controlled pore glass	21	(29)
Chitosan-halloysite hybrid-nanotubes	21.5	(30)
GO@Fe <sub>3</sub> O <sub>4</sub> @6arm-PEG-NH <sub>2</sub>	186.3	This work

GO=graphene oxide, PEG=polyethylene glycol

### Enzyme activity

**Fig. 5** shows the effect of various parameters on enzyme activity. The optimum pH of immobilized and free HRP was determined using different buffers with pH values of 5.5–8.5 and the results are shown in **Fig. 5a**. It can be seen that catalytic activities of immobilized HRP and free HRP reached the highest values at pH=7.5. This is consistent with the maximum activity of free HRP reported by Zhai *et al.* (30). In addition, when the pH was higher or lower than 7.5, the relative activity of the enzyme decreased. At higher pH, the relative activity of free HRP decreased more than of the immobilized HRP, which showed that the tolerance of immobilized HRP to the increased pH of the environment slightly improved. The

pH stability of HRP can be improved by loading the HRP onto the surface of GO@Fe<sub>3</sub>O<sub>4</sub>@6arm-PEG-NH<sub>2</sub> (31).

The optimum catalytic temperature of free and immobilized HRP was found to be 25 to 70 °C (**Fig. 5b**). The relative activity of the immobilized and free HRP increased with the increase of temperature and reached the maximum at 55 °C. The change of activity may be due to the gradual increase of the kinetic energy of the molecule with the increase of reaction temperature, and the increase of the collisional frequency between HRP and the substrate. As the temperature continued to rise, the relative activity of the enzyme began to decline, especially of the free HRP. This is attributed to too high temperature, causing the polypeptide that makes up the enzyme to deform, which reduces its activity.

### Kinetic parameters

The kinetic parameters ( $K_m$  and  $v_{max}$ ) of free HRP changed after immobilization on the support material. Specifically, the apparent  $K_m$  values of the free and immobilized HRP were 1.4525 and 0.6016 mmol/L, respectively. After immobilization, the  $v_{max}$  decreased slightly from 1230 to 1183  $\mu\text{M/s}$ . The lower  $K_m$  values of immobilized HRP suggested a higher affinity towards the phenolic substrate after immobilization. The change in the affinity of HRP to its substrate was maybe caused by structural changes in the enzyme.

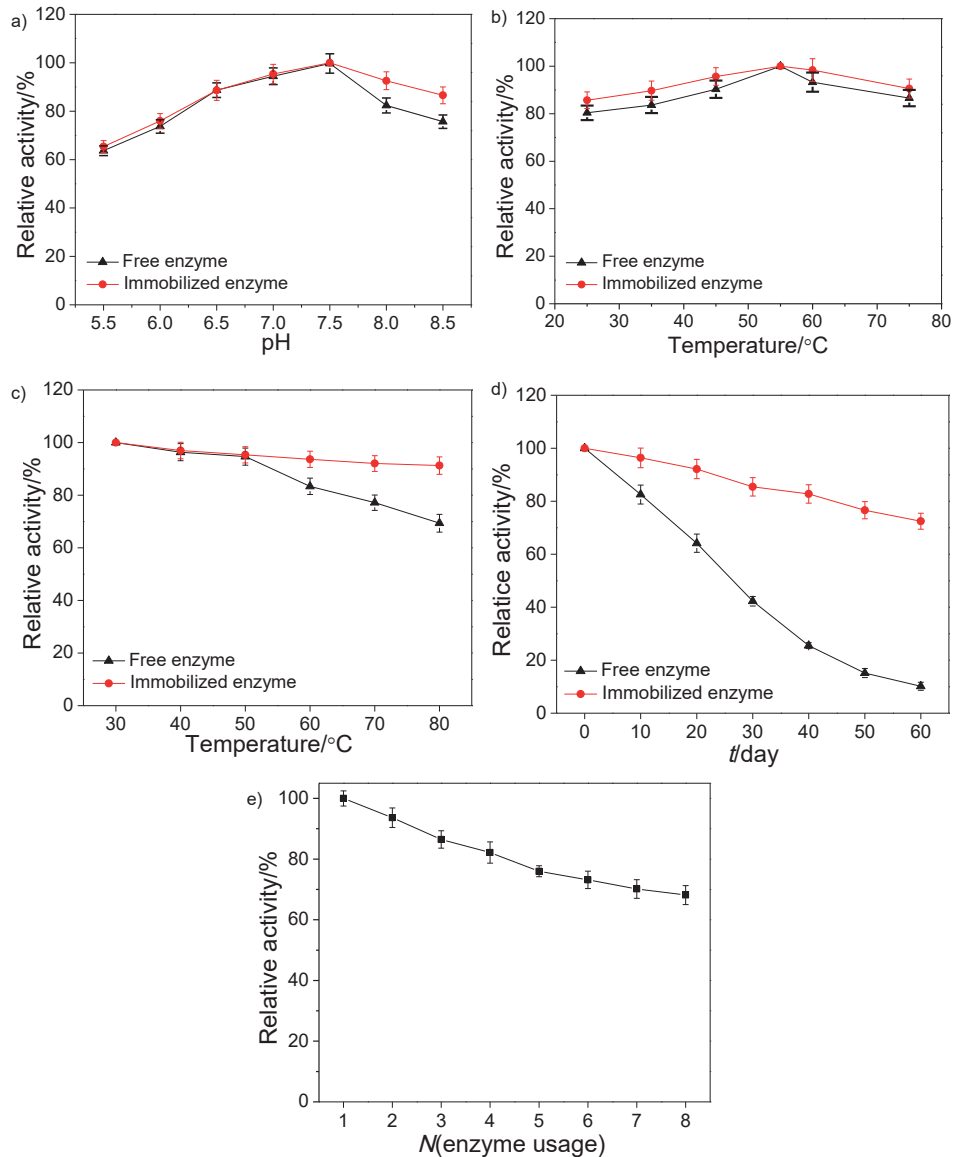


**Fig. 5.** Effect of: a) pH and b) temperature on the activity of free and immobilized horseradish peroxidase (HRP), c) thermal and d) storage stability of free and immobilized HRP, and e) reusability of immobilized HRP

### Thermal stability

The tolerance of immobilized HRP to temperature was investigated. **Fig. 5c** shows that the temperature increase from 30 to 80 °C caused gradual decrease of the enzyme activity. This may be due to the deformation of the polypeptide, which leads to inactivation of the HRP at high temperature. The thermal stability of the immobilized HRP greatly improved. Its activity was much higher than that of the free HRP at high temperature (80 °C).

### Storage stability

Stability of free and immobilized HRP during cold storage (4 °C) is shown in **Fig. 5d**. Under the same storage conditions,

the activity of immobilized HRP decreased more slowly than that of the free HRP. The relative activity of immobilized HRP after 30 days was 85.5 %, which was significantly higher than of free HRP (42.3 %). After 60 days, free HRP was almost completely inactivated (10.2 %), while the activity of immobilized HRP was still at a high level (72.5 %). It was concluded that the stability of HRP was enhanced by immobilization, which was in line with the thermal stability data (**Fig. 5c**). It was also concluded that the enzyme immobilized on GO@Fe<sub>3</sub>O<sub>4</sub>@6arm-PEG-NH<sub>2</sub> was more stable and had a longer shelf-life than other types of support materials (**Table 2** (32–34)).

**Table 2.** Relative activity of the immobilized horseradish peroxidase on different materials in storage stability studies

Immobilized support material	t(storage)/day	Residual activity/%	Reference
Starch	49	30	(32)
PSMAA	20	61	(33)
Graphene oxide (rGO-NH <sub>2</sub> )	35	60	(34)
GO@Fe <sub>3</sub> O <sub>4</sub> @6arm-PEG-NH <sub>2</sub>	60	72.5	This work

PSMAA=poly(styrene-co-methacrylic acid), rGO=reduced graphene oxide, PEG=polyethylene glycol

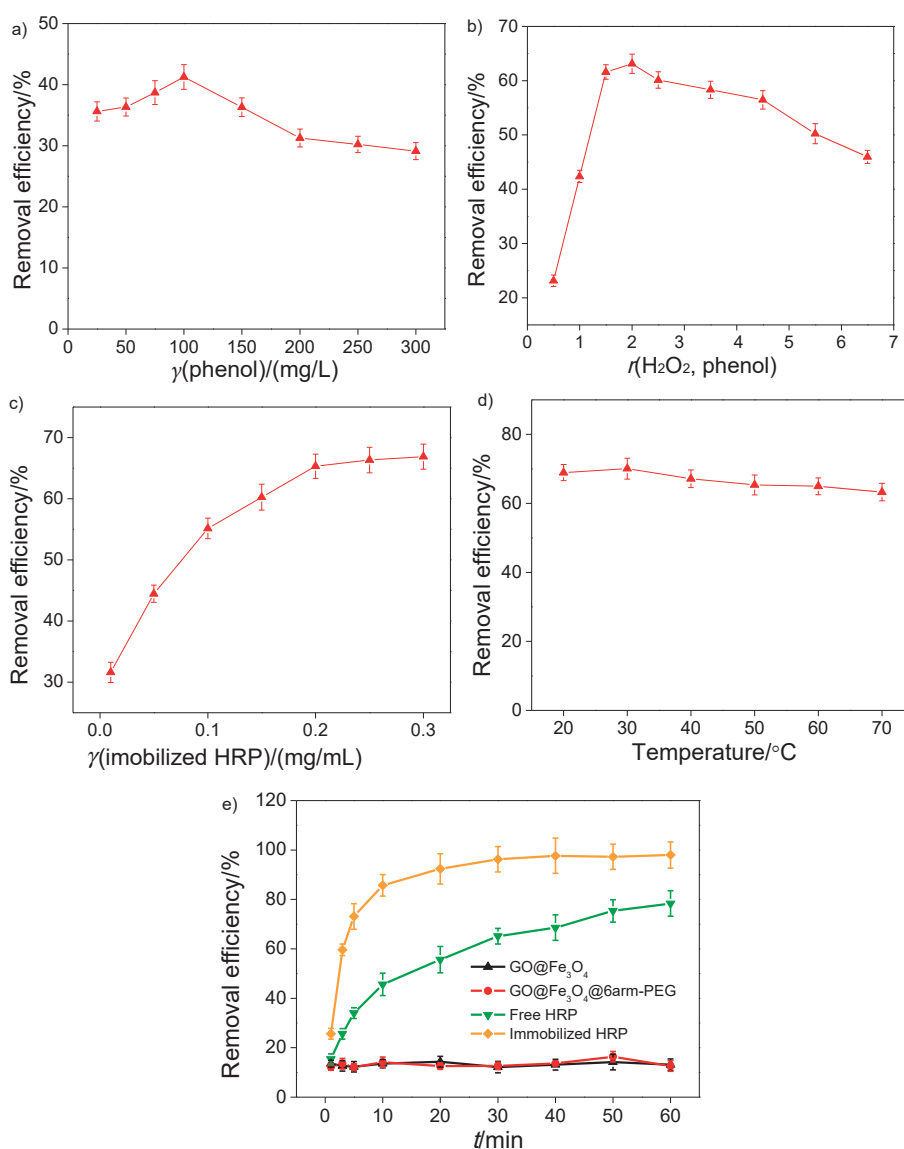
*Reusability of immobilized HRP*

Fig. 5e shows the reusability of immobilized HRP in eight catalysis runs. The activity of the immobilized HRP decreased with the increase of recycling number, and it was over 68.1 % of its initial value after eight cycles. The relative activity of

immobilized HRP reached 76.0 % after five cycles, and was significantly higher than 41 % on GO@Fe<sub>3</sub>O<sub>4</sub> as supporting material reported previously (35). This activity loss might be attributed to the accumulation of the products during the enzymatic reaction on the surface of the immobilized HRP, which blocked some of its reaction sites.

*Degradation of phenols by immobilized HRP*

Fig. 6 shows the effect of different reaction parameters, including concentrations of phenols, molar ratio of H<sub>2</sub>O<sub>2</sub> and phenols, concentration of immobilized HRP and reaction temperature on the degradation of phenols. Phenol removal efficiency increased rapidly with the increase of phenol concentration up to 100 mg/L, when it reached the maximum value of 41.26 % (Fig. 6a). However, when the concentration



**Fig. 6.** Effects of various reaction parameters on phenol removal efficiency: a) concentration of phenols, b) molar ratio of H<sub>2</sub>O<sub>2</sub> and phenols, c) concentration of immobilized horseradish peroxidase (HRP)d) temperature, and e) removal efficiency of immobilized HRP in comparison with free enzyme and support materials. PEG=polyethylene glycol

of phenols increased further, removal efficiency began to decline. This was due to the fact that the catalytic reaction rate was accelerated at first with the increase of substrate concentration, and when the substrate concentration was increased further, the aggregation of the product inhibited substrate degradation. Therefore, the phenol concentration of 100 mg/L was used as the optimum in the subsequent removal reaction.

The removal efficiency of phenols increased linearly with the increase of molar ratio of  $H_2O_2$  to phenols up to 2.0, when it reached 63.13 %, and then decreased (Fig. 6b). The reason for this could be that too much  $H_2O_2$  causes excessive oxidation of the iron ions at the centre of HRP activity and affect the transmission of electrons, which may prevent catalytic reaction. Therefore, the optimal molar ratio of  $H_2O_2$  to phenol was determined to be 2.0.

Fig. 6c shows that phenol removal efficiency increased rapidly with the increase of the concentration of immobilized HRP up to 0.2 mg/L, when it started to decrease. Based on the above findings, the optimal concentration of immobilized HRP was found to be 0.2 mg/L.

The effect of different reaction temperatures on the phenol removal efficiency was studied (Fig. 6d), and we concluded that it was not significant. Phenol removal efficiency decreased slightly with the increase of reaction temperature. Considering the thermal stability of immobilized HRP, optimal reaction temperature was determined to be 20 °C.

#### *Synergistic effect between HRP and GO@Fe<sub>3</sub>O<sub>4</sub>@6arm-PEG-NH<sub>2</sub> during phenol degradation*

The degradation of phenols (100 mg/L) by the catalytic activity of immobilized HRP, free HRP, GO@Fe<sub>3</sub>O<sub>4</sub> and GO@Fe<sub>3</sub>O<sub>4</sub>@6arm-PEG-NH<sub>2</sub> in the presence of  $H_2O_2$  (1.59 mmol/L) at pH=7.5 and 20 °C was investigated. Fig. 6e shows that the degradation rate of phenols by immobilized HRP was 85.7 % after 10 min, while by the free HRP, GO@Fe<sub>3</sub>O<sub>4</sub> and GO@Fe<sub>3</sub>O<sub>4</sub>@6arm-PEG-NH<sub>2</sub>, it was 45.6, 13.5 and 14.1 % respectively. The relative activity of the pure carrier material was very weak because there was only non-specific adsorption effect between the carrier and the phenols. It indicated that the degradation of phenols by immobilized HRP was significantly better than by free enzyme and support material alone, due to the synergistic effect between the HRP and the support material, which is consistent with the previous literature report (26).

## CONCLUSIONS

In this work we synthesized a novel type of the magnetic multi-arm nanocomposite GO@Fe<sub>3</sub>O<sub>4</sub>@6arm-PEG-NH<sub>2</sub> and applied it for the immobilization of horseradish peroxidase (HRP). The efficient degradation of phenols was achieved by using HRP and GO@Fe<sub>3</sub>O<sub>4</sub>@6arm-PEG-NH<sub>2</sub> as a binary enzymatic catalyst and  $H_2O_2$  as an oxidant. Significant improvements in HRP stability and oxidation of phenols were observable after immobilization on GO@Fe<sub>3</sub>O<sub>4</sub>@6arm-PEG-NH<sub>2</sub>, in

addition to high reusability. The loading of HRP was comparably higher than of previously reported supports for HRP. Compared with the free enzyme, thermal, storage and operational stabilities of the immobilized HRP have improved. The activity of the immobilized HRP was still over 68.1 % after eight cycles. The removal efficiency of phenols by immobilized HRP was significantly better than that of free enzyme and support material. The synergistic effect of the two catalysts can significantly improve the efficiency of phenol removal. These results suggest that the multi-armed magnetic composite has a good potential for enzyme immobilization.

## ACKNOWLEDGEMENTS

This work was supported by the National Natural Science Foundation of China (project nos. 21676124, 21878131 and 21576124), and China Postdoctoral Science Foundation (project no. 2017M610308).

## CONFLICT OF INTEREST

There are no conflicts of interest to declare.

## ORCID IDs

J. Rong  <https://orcid.org/0000-0002-3115-6476>

Z. Zhou  <https://orcid.org/0000-0001-6579-3230>

Y. Wang  <https://orcid.org/0000-0003-0024-0824>

J. Han  <https://orcid.org/0000-0001-9472-0647>

C. Li  <https://orcid.org/0000-0003-0261-5343>

W. Zhang  <https://orcid.org/0000-0001-8084-1456>

L. Ni  <https://orcid.org/0000-0002-6463-7823>

## REFERENCES

1. Alemzadeh I, Nejati S. Phenols removal by immobilized horseradish peroxidase. *J Hazard Mat.* 2009;166(2-3):1082–6. <https://doi.org/10.1016/j.jhazmat.2008.12.026>
2. Kim GY, Lee KB, Cho SH, Shim J, Moon SH. Electroenzymatic degradation of azo dye using an immobilized peroxidase enzyme. *J Hazard Mat.* 2005;126(1-3):183–8. <https://doi.org/10.1016/j.jhazmat.2005.06.023>
3. Rathner R, Petz S, Tasnádi G, Koller M, Ribitsch V. Monitoring the kinetics of biocatalytic removal of the endocrine disrupting compound 17 $\alpha$ -ethinylestradiol from differently polluted wastewater bodies. *J Environ Chem Eng.* 2017; 5(2):1920–6. <https://doi.org/10.1016/j.jece.2017.03.034>
4. Huang Q, Huang Q, Pinto RA, Griebenow K, Schweitzer-Stenner R, Weber WJ. Inactivation of horseradish peroxidase by phenoxyl radical attack. *J Am Chem Soc.* 2005;127(5):1431–7. <https://doi.org/10.1021/ja045986h>
5. Cheng J, Yu SM, Zuo P. Horseradish peroxidase immobilized on aluminium-pillared inter-layered clay for the

- catalytic oxidation of phenolic wastewater. *Water Res.* 2006; 40(2):283–90.  
<https://doi.org/10.1016/j.watres.2005.11.017>
6. Sadjadi MS, Farhadyar N, Zare K. Preparation of core-shell ZnO-SiO<sub>2</sub> nanowires-nanotubes for immobilization of the alkaline protease enzyme. *J Nanosci Nanotechnol.* 2011; 11(10):9304–9.  
<https://doi.org/10.1166/jnn.2011.4312>
  7. Mohan T, Rathner R, Reishofer D, Koller M, Elschner T, Spirk S, *et al.* Designing hydrophobically modified polysaccharide derivatives for highly efficient enzyme immobilization. *Biomacromolecules.* 2015;16(8):2403–11.  
<https://doi.org/10.1021/acs.biomac.5b00638>
  8. Zang L, Qiu J, Wu X, Zhang W, Sakai E, Wei Y. Preparation of magnetic chitosan nanoparticles as support for cellulase immobilization. *Ind Eng Chem Res.* 2014;53(9):3448–54.  
<https://doi.org/10.1021/ie404072s>
  9. Guo H, Tang Y, Yu Y, Xue L, Qian JQ. Covalent immobilization of  $\alpha$ -amylase on magnetic particles as catalyst for hydrolysis of high-amylose starch. *Int J Biol Macromol.* 2016;87:537–44.  
<https://doi.org/10.1016/j.ijbiomac.2016.02.080>
  10. Yang D, Wang X, Shi J, Wang X, Zhang S, Han P, Jiang Z. *In situ* synthesized rGO-Fe<sub>3</sub>O<sub>4</sub> nanocomposites as enzyme immobilization support for achieving high activity recovery and easy recycling. *Biochem Eng J.* 2016;105(Part A):273–80.  
<https://doi.org/10.1016/j.bej.2015.10.003>
  11. Fowler JD, Allen MJ, Tung VC, Yang Y, Kaner RB, Weiller BH. Practical chemical sensors from chemically derived graphene. *ACS Nano.* 2009;3(2):301–6.  
<https://doi.org/10.1021/nn800593m>
  12. Li D, Müller MB, Gilje S, Kaner RB, Wallace GG. Processable aqueous dispersions of graphene nanosheets. *Nat Nanotechnol.* 2008;3(2):101–5.  
<https://doi.org/10.1038/nnano.2007.451>
  13. Song Y, Qu K, Zhao C, Ren J, Qu X. Graphene oxide: Intrinsic peroxidase catalytic activity and its application to glucose detection. *Adv Mater.* 2010;22(19):2206–10.  
<https://doi.org/10.1002/adma.200903783>
  14. Wang M, Wang N, Tang H, Cao M, She Y, Zhu L. Surface modification of nano-Fe<sub>3</sub>O<sub>4</sub> with EDTA and its use in H<sub>2</sub>O<sub>2</sub> activation for removing organic pollutants. *Catal Sci Technol.* 2012;2(1):187–94.  
<https://doi.org/10.1039/c1cy00260k>
  15. Wang N, Zhu L, Wang M, Wang D, Tang H. Sono-enhanced degradation of dye pollutants with the use of H<sub>2</sub>O<sub>2</sub> activated by Fe<sub>3</sub>O<sub>4</sub> magnetic nanoparticles as peroxidase mimetic. *Ultrason Sonochem.* 2010;17(1):78–83.  
<https://doi.org/10.1016/j.ultsonch.2009.06.014>
  16. Taleb KA, Rusmirović JD, Rančić MP, Nikolić JB, Drmanić SZ, Veličković Zlate Z, Marinković AD. Efficient pollutants removal by amino-modified nanocellulose impregnated with iron oxide. *J Serb Chem Soc.* 2016;81(10):1199–213.  
<https://doi.org/10.2298/Jsc160529063t>
  17. Hummers Jr WS, Offeman RE. Preparation of graphitic oxide. *J Am Chem Soc.* 1958;80(6):1339.  
<https://doi.org/10.1021/ja01539a017>
  18. Chang Q, Tang H. Optical determination of glucose and hydrogen peroxide using a nanocomposite prepared from glucose oxidase and magnetite nanoparticles immobilized on graphene oxide. *Microchim Acta.* 2014;181(5-6):527–34.  
<https://doi.org/10.1007/s00604-013-1145-x>
  19. Iida H, Takayanagi K, Nakanishi T, Osaka T. Synthesis of Fe<sub>3</sub>O<sub>4</sub> nanoparticles with various sizes and magnetic properties by controlled hydrolysis. *J Colloid Interface Sci.* 2007;314(1): 274–80.  
<https://doi.org/10.1016/j.jcis.2007.05.047>
  20. Zhuang W, He L, Zhu J, Zheng J, Liu X, Dong Y, *et al.* Efficient nanobiocatalytic systems of nuclease P<sub>1</sub> immobilized on PEG-NH<sub>2</sub> modified graphene oxide: Effects of interface property heterogeneity. *Colloid Surf B Biointerfaces.* 2016; 145:785–94.  
<https://doi.org/10.1016/j.colsurfb.2016.05.074>
  21. Bradford MM. A rapid and sensitive method for the quantitation of microgram quantities of protein using the principle of protein-dye binding. *Anal Biochem.* 1976;72(1-2):248–54.  
[https://doi.org/10.1016/0003-2697\(76\)90527-3](https://doi.org/10.1016/0003-2697(76)90527-3)
  22. Han J, Cai Y, Wang Y, Gu L, Li CM, Mao Y, *et al.* Synergetic effect of Ni<sup>2+</sup> and 5-acrylamidobenzoboroxole functional groups anchoring on magnetic nanoparticles for enhanced immobilization of horseradish peroxidase. *Enzyme Microb Technol.* 2019;120:136–43.  
<https://doi.org/10.1016/j.enzmictec.2018.06.002>
  23. Saito Y, Nakashima S, Mifune M, Odo J, Tanaka Y, Chikuma M, Tanaka H. Determination of hydrogen peroxide by use of an anion-exchange resin modified with manganese tetrakis (sulfophenyl) porphine as a mimesis of peroxidase. *Anal Chim Acta.* 1985;172:285–7.  
[https://doi.org/10.1016/S0003-2670\(00\)82616-1](https://doi.org/10.1016/S0003-2670(00)82616-1)
  24. International Centre for Diffraction Data (ICDD), Newton Square, PA, USA; 2019. Available from: [www.icdd.com](http://www.icdd.com).
  25. Matsumoto Y, Koinuma M, Kim SY, Watanabe Y, Taniguchi T, Hatakeyama K, *et al.* Simple photoreduction of graphene oxide nanosheet under mild conditions. *ACS Appl Mater Interfaces.* 2010;2(12):3461–6.  
<https://doi.org/10.1021/am100900q>
  26. Huang J, Chang Q, Ding Y, Han X, Tang H. Catalytic oxidative removal of 2,4-dichlorophenol by simultaneous use of horseradish peroxidase and graphene oxide/Fe<sub>3</sub>O<sub>4</sub> as catalyst. *Chem Eng J.* 2014;254(7):434–42.  
<https://doi.org/10.1016/j.cej.2014.05.136>
  27. Lai YC, Lin SC. Application of immobilized horseradish peroxidase for the removal of *p*-chlorophenol from aqueous

- solution. *Process Biochem.* 2005;40(3-4):1167–74.  
<https://doi.org/10.1016/j.procbio.2004.04.009>
28. Gómez JL, Bódalo A, Gómez E, Bastida J, Hidalgo AM, Gómez M. Immobilization of peroxidases on glass beads: An improved alternative for phenol removal. *Enzyme Microb Technol.* 2006;39(5):1016–22.  
<https://doi.org/10.1016/j.enzmictec.2006.02.008>
29. Azevedo AM, Vojinović V, Cabral JMS, Gibson TD, Fonseca LP. Operational stability of immobilised horseradish peroxidase in mini-packed bed bioreactors. *J Mol Catal B Enzym.* 2004;28(2-3):121–8.
30. Zhai R, Zhang B, Wan Y, Li C, Wang J, Liu J. Chitosan-halloysite hybrid-nanotubes: Horseradish peroxidase immobilization and applications in phenol removal. *Chem Eng J.* 2013;214:304–9.  
<https://doi.org/10.1016/j.cej.2012.10.073>
31. Ai J, Zhang W, Liao G, Xia H, Wang D. Immobilization of horseradish peroxidase enzymes on hydrous-titanium and application for phenol removal. *RSC Adv.* 2016;6(44):38117–23.  
<https://doi.org/10.1039/c6ra02397e>
32. Kagliwal LD, Singhal RS. Enzyme-polysaccharide interaction: A method for improved stability of horseradish peroxidase. *Int J Biol Macromol.* 2014;69(8):329–35.  
<https://doi.org/10.1016/j.ijbiomac.2014.05.065>
33. Pan C, Ding R, Dong L, Wang J, Hu Y. Horseradish peroxidase-carrying electrospun nonwoven fabrics for the treatment of *o*-methoxyphenol. *J Nanomater.* 2015;2015:Article ID 616879.  
<https://doi.org/10.1155/2015/616879>
34. Vineh MB, Saboury AA, Poostchi AA, Mamani L. Physical adsorption of horseradish peroxidase on reduced graphene oxide nanosheets functionalized by amine: A good system for biodegradation of high phenol concentration in wastewater. *Int J Environ Res.* 2018;12(1):45–57.  
<https://doi.org/10.1007/s41742-018-0067-1>
35. Chang Q, Huang J, Ding Y, Tang H. Catalytic oxidation of phenol and 2,4-dichlorophenol by using horseradish peroxidase immobilized on graphene oxide/Fe<sub>3</sub>O<sub>4</sub>. *Molecules.* 2016;21(8):1044.  
<https://doi.org/10.3390/Molecules21081044>